

Human Movement Sciences Sport, Exercise & Health (research)

Research Internship Research Master 2014-2015
(course code FBW_B_RIRM_2014_001)

EEG source localization of P50 and P100 in healthy subjects and chronic stroke patients.

A pilot study to examine the possible value of the location and orientation of primary and secondary somatosensory cortex to predict upper limb recovery after stroke.



DINSDAG 14 APRIL 2015

Algemeen **9**

Binnenland

Gevolgen en herstel beroerte in kaart brengen

mogelijk, maar de apparatuur wordt steeds kleiner.
De bus bezoekt de patiënten na 1, 2, 3, 4, 5, 8, 12 en 26 weken na een beroerte om het verloop van herstel in kaart te brengen. Daarbij moet de patiënt (die doorgaans uitvalverschijnselen aan één kant heeft) met een soort robot oefeningen doen, met zijn verlamde arm. De EEG registreert hoe de hersenen reageren op die activiteiten van de spieren. „De kwaliteit waarmee het signaal terugkomt naar de hersenen, zegt iets over de herstel-mogelijkheden”, aldus Kwakkel.

Activeren
Lange tijd werd gedacht dat elektrostimulatie van spieren de verlammingen na een beroerte weer zou kunnen helpen opheffen, maar dat blijkt niet waar, zegt Kwakkel. Waar wel goede resultaten mee werden geboekt, is het immobiliseren van de gezonde arm, waardoor mensen als het ware gedwongen worden de verlamde arm te activeren. „Cru gezegd: use it or lose it. Ook dat volgen we met de EEG. Het is interessant om te zien wat er in de hersenen verandert als een verlamde arm herstelt. Wordt dat overgenomen door de gezonde hersenhelft waar je dan soms verhoogde hersenactiviteit ziet en hoe ontwikkelt dat zich in de tijd. Op dat soort vragen zoeken we allemaal antwoorden.”

Bewegingswetenschapper Gert Kwakkel van VUmc en onderzoeker Caroline Winters met een proefpersoon in de hersenenmeter. FOTO ELLA TILGENKAMP

Hersenenmeter komt langs

Rien Floris
rienfloris@hivemind.com

Amsterdam * De hersenenmeter, een project van VUmc en de TU Delft, start volgende week met het grootste EEG-onderzoek ooit gehouden bij patiënten met een beroerte. „Door intensief en veel te meten, kun je veel meer te weten komen over de verwachtingen voor herstel”, zegt bewegingswetenschapper (hoogleraar neurorevalidatie) Gert Kwakkel van VU medisch centrum. Hij coördineert het project. Jaarlijks worden 174.000 mensen getroffen door een beroerte. „Binnen een paar uur kun je er vaak nog iets aan doen, maar daarna is revalidatie het enige traject dat nog voor verbetering kan zorgen”, zegt Kwakkel.

Vijf dagen
Binnen vijf dagen wordt een patiënt die een beroerte gehad heeft, doorgaans ontslagen uit het ziekenhuis, maar herstel kan maanden tot jaren duren. De vooruitzichten voor patiënten zijn heel verschillend; van weinig schade tot blijvende halfzijdige verlamming. Wat zijn de verwachtingen en helpt het als je al vroeg begint met revalideren? De hersenenmeter doet hersenscans (EEG) en gaat antwoord zoeken op die vragen, zodat artsen hopelijk gerichte revalidatie kunnen inzetten. Volgende week is de eerste patiënt aan de beurt, maar er moet nog heel veel worden gemeten in Noord- en Zuid-Holland. „Nu kan niemand goed in kaart brengen hoe het verloop bij een beroerte is omdat de patiënten in een zorgtraject verdwijnen. De een zit thuis met hulp, de ander in een revalidatiekliniek en een volgende in een verpleeghuis”, zegt Kwakkel. Daarom is het niet doelmiddel om het onderzoek in VUmc te doen, dus gaat de bus de regio in. Bovendien is de bus die geheel ingericht is met apparatuur voor een EEG (elektro-encefalografie), veel goedkoper dan alle patiënten per taxi naar VUmc te laten komen. Bovendien is het voor de patiënt minder belastend als hij niet hoeft te reizen. „Vijf jaar geleden was dit niet

VU University Amsterdam
Faculty of Human Movement Sciences
Qualification: MSc in Human Movement Sciences
Research internship Research Master

Author:
H.E. van Dorp, BSc

Supervisors:
C. Winters, MSc; Dr. E.E.H. van Wegen; Prof. Dr. A. Daffertshofer

August, 2015

Summary

Objectives: The measurement of somatosensory evoked potentials (SEPs) with electroencephalography (EEG) may serve as a useful tool to predict upper limb recovery post stroke. Few studies have examined the predictive value of SEPs at source level. The aim of the present study was therefore to examine the difference in location and orientation between the source of the P50 SEP-component and that of the P100 SEP-component in healthy subjects and chronic stroke patients. P50 and P100 were expected to be located in, respectively, the primary and secondary somatosensory cortex, making them excellent candidates for predicting upper limb recovery post stroke.

Methods: 10 young and 4 older healthy subjects and 4 chronic stroke patients were included in the study. SEPs were evoked by electrical stimulation of the index finger of the dominant hand for healthy subjects and the affected hand for patients and were recorded using 62-channel EEG. In addition, three-dimensional T1-weighted MR images were obtained for all subjects.

Analysis: A single equivalent moving dipole was applied to the whole time period and a hierarchical clustering approach was used to separate dipole locations belonging to P50 and P100 components. Subsequently, a single dipole model was applied to the periods in which the selected clusters were active and the difference in location and orientation between the subject-specific P50 and P100 sources was determined and compared between groups.

Results: While the P50 and P100 sources did appear at separate location for all subjects, for most of them the sources were not located in SI and SII, respectively. Moreover, no differences were found when the difference in location and orientation between the sources of P50 and P100 was compared between groups.

Conclusions: The present study did reveal two subject-specific dipolar sources for the P50 and P100 component. In contrast to the expectation, these sources were not consistently located in SI and SII, respectively, making their predictive value for upper limb recovery post stroke unclear.

Key words: *Stroke; recovery; somatosensory evoked potential (SEP); electroencephalography (EEG); source analysis*

Content

1	Introduction	3
2	General background.....	5
3	Methods & Procedures.....	8
3.1	Subjects	8
3.2	Procedures.....	8
3.3	Data acquisition.....	8
3.3.1	Clinical assessments.....	8
3.3.2	Neurophysiological examination.....	8
3.3.3	EEG recordings.....	9
3.4	Data analysis	9
3.4.1	Preprocessing.....	9
3.4.2	Sensor level analysis	10
3.4.3	Source localization.....	10
3.4.4	The source parameters	11
3.5	Statistical analysis	12
4	Results.....	12
4.1	Demographic data and clinical characteristics.....	12
4.2	Amplitude and post-stimulus latency.....	13
4.3	Source localization	14
4.3.1	Young healthy subjects	14
4.3.2	Older healthy subjects.....	18
4.3.3	Chronic stroke patients.....	18
4.4	Difference in location and orientation	20
5	Discussion	20
6	Conclusions.....	24
7	Acknowledgements	24
8	References.....	25

1 Introduction

Stroke (infarction or hemorrhage) is one of the leading causes of death and long-term disability in the Western countries. In the Netherlands the lifetime risk of suffering a stroke is around 21% in people older than 55 years of age (Hollander *et al.*, 2003). Stroke is caused by a critical reduction in the blood supply to a particular part of the brain, leading to structural damage of neurons (Hossmann, 2006). The resulting impairment of motor and sensory function is dependent on the location and extent of the lesion. Motor impairment of the upper limb is one of the most common deficits among stroke survivors and recovery is generally poor. Less than 15% of the stroke patients with initial paralysis of the upper limb show complete motor recovery (for review see Hendricks *et al.*, 2002).

Almost all stroke patients show at least some degree of improvement over time, particularly in the first 6 to 10 weeks after stroke onset (Kwakkel *et al.*, 2006). The processes underlying motor recovery after stroke may be described as either restitution or substitution of body function. The restitution model assumes that improvement in body function is caused by true neurological recovery (i.e. plasticity), while the substitution model suggests that functional improvement is mainly a result of adaptation or behavioral compensation strategies (van Kordelaar *et al.*, 2013; Rothi & Horner, 1982). Although both processes occur during the course of recovery, one may suggest that restitution of body function is dominant in the early period post stroke (for review see Buma *et al.*, 2013; van Kordelaar *et al.*, 2013). In this early period spontaneous neurological recovery and learning dependent mechanisms of neuroplasticity are thought to take place, which have been suggested to lead to restoration of neural circuits and contributes to restitution of body function (for review see Murphy & Corbett, 2009). After this time window of enhanced plasticity, recovery levels off and it is presumed that substitution of body function is the predominant mechanism underlying further functional improvement (for review see Buma *et al.*, 2004; Kwakkel *et al.*, 2006).

Knowledge about the duration and extent of enhanced cortical plasticity provides the opportunity to predict outcome of upper limb function early post stroke (Kwakkel *et al.*, 2006). A reliable prediction of the extent of upper limb recovery would enable physical therapists to focus their therapy on either the restoration of the existing deficits or on the use of certain compensation strategies. Currently, the algorithms predicting upper limb recovery after stroke are often based on clinical assessments. Shoulder abduction and finger extension measured within 72 hours after stroke, for instance, are strongly related to recovery of upper limb function after 6 months (Nijland *et al.*, 2010). Patients with some finger extension and shoulder abduction 2 days post stroke had a probability of 98% to achieve some dexterity at 6 months. However, a number of patients with initially no voluntary motor control still recovered some dexterity at 6 months (Nijland *et al.*, 2010). For a more accurate prediction of upper limb recovery in this group of patients refinement of the existing algorithms is necessary. The addition of neurophysiological measures, like somatosensory evoked potentials (SEPs) recorded with electroencephalography (EEG), may improve the predictive accuracy. Both the motor and somatosensory pathways, as well as the interaction between these pathways, are important for an adequate function of the upper limb (Rothwell *et al.*, 1982). The SEP can be generated by electrical stimulation of the median nerve at the wrist or of the fingertip and it is therefore an objective and quantitative measure.

Several studies have investigated the possible value of early cortical SEPs, generated by median nerve stimulation, to predict upper limb recovery and overall functional recovery (Al-Rawi *et al.*, 2009; Feys *et al.*, 2000; Hendricks *et al.*, 1994; Hendricks *et al.*, 1997; Keren *et al.*, 1993; Péréon *et*

al., 1995; Timmerhuis *et al.*, 1996; Tzvetanov & Rousseff, 2003). The early cortical SEPs are believed to be primarily generated in the contralateral primary somatosensory cortex (SI) (Allison *et al.*, 1989a; Forss *et al.*, 1994; Hämäläinen *et al.*, 1990). SI is located in the postcentral sulcus and in the depths of the central sulcus (Woolsey *et al.*, 1979) and predominantly encodes the perception of stimulus intensity, location and duration (Schnitzler & Ploner, 2000). In addition, SI has direct projections to the primary motor cortex (M1) and is an important source of somatosensory input to M1 (Jones *et al.*, 1978). Early cortical median nerve SEPs occur between 20 and 40 ms after stimulus onset (Allison *et al.*, 1989a; Forss *et al.*, 1994), while for finger stimulation the first reliable responses in SI are present after 50 ms (Forss *et al.*, 2012; Hämäläinen *et al.*, 1990). Although two studies revealed limited predictive value of early SEPs (Péréon *et al.*, 1995; Timmerhuis *et al.*, 1996), others reported that early SEPs correlate well with the level of disability (Al-Rawi *et al.*, 2009; Feys *et al.*, 2000; Hendricks *et al.*, 1994; Hendricks *et al.*, 1997; Keren *et al.*, 1993; Tzvetanov & Rousseff, 2003). All of these studies found that absence of early cortical SEPs in the acute phase post stroke is a strong indicator of poor (upper limb) recovery. According to the study of Hendricks and colleagues (1997), for instance, no motor recovery occurred in 89% of the patients without visible SEPs in the subacute phase post stroke. When SEPs were present 45% of the patients showed some degree of motor recovery 1 to 4 years post stroke.

When the early cortical SEPs are present conclusions about the predictive value of the SEP variables, like amplitude and latency, are still inconsistent. Some studies found that both reduced amplitude and prolonged latency of the early SEPs are correlated with poor motor recovery (Al-Rawi *et al.*, 2009; Keren *et al.*, 1993), while other studies did only find this relation for the SEP amplitude (Tzvetanov & Rousseff, 2003), or did not find a difference at all between patients with abnormal and normal SEPs (Feys *et al.*, 2000). This inconsistency may be due to the different outcome measures and follow-up times used in these studies.

The long-latency SEPs, which occur after 40 ms for median nerve stimulation (Allison *et al.*, 1989b) and after 70 ms for finger stimulation (Desmedt & Robertson, 1977), have received little attention in stroke research. In this time period other regions in the parietal cortex are activated in addition to SI (Allison *et al.*, 1989b; Forss *et al.*, 1994; Hämäläinen *et al.*, 1990). SEP-components peaking at around 100 to 140 ms after stimulus onset have been recorded from the secondary somatosensory cortices (SII) in both hemispheres (Allison *et al.*, 1989b; Hämäläinen *et al.*, 1990). SII is located lateral and posterior to SI in the upper bank of the Sylvian fissure, also called the parietal operculum (Woolsey *et al.*, 1979). Bilateral activation of SII is thought to be involved in the execution of higher-order functions, like sensorimotor integration (Disbrow *et al.*, 2000) and attention (Burton *et al.*, 1999). Few reports have assessed the long-latency SEPs in stroke patients and found reduced amplitudes and increased latencies after electrical stimulation of the median nerve (Yuya *et al.*, 1996) and finger (Roosink *et al.*, 2011) of the affected side. In addition, Forss and colleagues (2012) found correlations between the amplitude of the response in SII and hand function in the acute phase as well as three months post stroke. They did not find a correlation between the amplitude and latency of the SI response and hand function. Thus, it remains unclear whether the amplitude and/or latency of the early and/or late cortical SEPs can be used as reliable predictors of upper limb recovery after stroke.

Most EEG studies investigating the predictive value of SEP examined the SEP-components at sensor level. Moreover, some studies investigated the electrical potentials from only a few electrodes placed over the contralateral somatosensory areas (Al-Rawi *et al.*, 2009; Feys *et al.*, 2000; Hendricks *et al.*, 1994; Hendricks *et al.*, 1997; Keren *et al.*, 1993; Péréon *et al.*, 1995; Timmerhuis *et al.*, 1996; Tzvetanov & Rousseff, 2003). Nevertheless, the electrical potentials measured on the scalp do not directly reflect the location of the active sources in the brain (Nunez, 1981). When

more electrodes are used the location, orientation and strength of the sources can be estimated from the potential distribution on the scalp by the introduction of various a priori assumptions (Fender, 1987). These source parameters may serve as useful predictors of upper limb recovery, in particular if they agree with SI and SII coordinates. After stroke SI is assumed to undergo plastic reorganization, which is reflected by a topographical shift of the generator sources of the early SEPs in the chronic phase post stroke (Rossini *et al.*, 2001). It is suggested that SII also has the capacity for plastic reorganization (Pons *et al.*, 1988). As said, it is believed that SI and SII are activated in a serial way (Hu *et al.*, 2012; Inui *et al.*, 2004) and have different functions during the processing of somatosensory information (Burton *et al.*, 1999; Disbrow *et al.*, 2000; Schnitzler & Ploner, 2000). However, since SI and SII are assumed to have a functional overlap in somatotopy (Simoës *et al.*, 2001) one area might be able to compensate for structural damage of neurons in the other area. This may affect the location and orientation of the generating sources of the early and late SEP-components.

The aim of the present study was to locate and separate the cortical sources of the P50 and P100 SEP-component after electrical stimulation of the index finger in healthy subjects and in chronic stroke patients. Subsequently, the difference in location and orientation between the P50 and P100 source was examined and compared between both groups. The difference in location and orientation between the P50 and P100 source was expected to be smaller in stroke patients than in healthy subjects. When one of the sources has (partially) taken over the function of the other, the difference in location and orientation between the sources will become smaller. Furthermore, P50 and P100 were expected to be located in, respectively, SI and SII, making them excellent candidates for predicting upper limb recovery post stroke. This study serves as an explorative study for further research into the predictive value of SEPs. In a longitudinal study the possible predictors presented in this study can be examined over time in the early period post stroke and can be correlated with upper limb function.

2 General background

SEPs are generated by electrical stimulation of the afferent peripheral nerve fibers. For upper limb SEPs electrical pulses are transcutaneous delivered to the median nerve at the wrist or to one of the fingertips (Nuwer, 1998). After delivery of the stimulus a volley of action potentials will travel along the afferent nerve fibers to the shoulder, neck and scalp, which can be recorded as a series of positive and negative potentials. The SEP components can be identified by its archetypical waveform and can be quantified in terms of post-stimulus latency, amplitude and interpeak interval (Cruccu *et al.*, 2008). To label the different SEP components N or P is used to indicate the presumed polarity (negative or positive), followed by an integer to denote the typical latency (in ms) in healthy adults, for example P50 denotes a positive surface potential at around 50 ms after stimulus onset.

One of the earliest detectable SEP-components arises in the shoulder, in the brachial plexus region. This component is called the Erb's point peak or N9. Subsequently, the sensory fibers join the posterior columns of the spinal cord and synapse in the midcervical spinal cord, which can be recorded at the fifth or seventh cervical spine as N13. Around the same time a far-field potential (P14), arising from a region close to the cervico-medullary junction, can be recorded from the scalp. When the nerve impulses are further transmitted into the upper midbrain and thalamus a N18 far-field potential can be recorded. Eventually, the nerve impulses will arrive in the somatosensory cortex (for review see Nuwer, 1998). These cortical SEP-components can be recorded and localized using EEG.

Since the median nerve is a mixed sensory-motor nerve, electrical stimulation of the median nerve will activate both the motor and somatosensory areas (Huang *et al.*, 2004). During finger stimulation the digital nerves are excited, which branches from the median nerve and only contain afferent nerve fibers. It is therefore assumed that finger stimulation only evokes a somatosensory response. Despite these differences between median nerve and finger stimulation the cerebral responses in the somatosensory areas are similar in configuration. The cerebral response is only smaller in amplitude and longer in latency after stimulation of the finger. In addition, the different SEP-components are better defined for median nerve stimulation (Calmes & Cracco, 1971). Because finger stimulation is assumed to evoke a localized response in only the somatosensory areas it was decided to use finger stimulation in the present study. Figure 1 provides an example of the cortical SEP after stimulation of the left middle finger. As can be seen in this figure, the early (P50) and late (N70, P100, N140) SEP-components were most clearly present in the postcentral region of the right hemisphere.

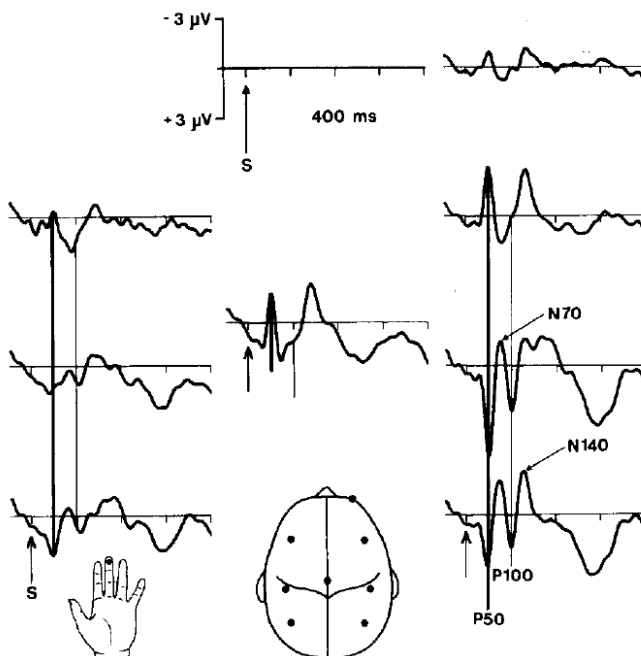


Figure 1. The cortical SEP after electrical stimulation of the left middle finger recorded at different locations on the left and right hemisphere. (from Hämäläinen *et al.*, 1990)

EEG signals are primarily generated by postsynaptic ionic currents of pyramidal neurons in the cortex which are synchronously active (Babiloni *et al.*, 2009). During the processing of incoming information from thalamus and brainstem active neurons produce small electrical currents across their cell membranes. These so-called action potentials will propagate from the cell body of the neuron to the axon terminals, producing a post-synaptic potential. Although post-synaptic potentials are longer lasting than action potentials they cannot be detected by EEG, because they are very small and the signal-to-noise ratio for the recording is poor. However, cortical pyramidal neurons are arranged in organized layers and they are all oriented perpendicularly to the scalp surface, which makes them suitable for the spatial summation of the post-synaptic potentials. Synchronous activity of the cortical pyramidal cells will result in an electrical potential that is measurable at the scalp.

Unfortunately, the measured electrical potentials on the scalp surface do not directly reflect the location of the active sources in the brain. While EEG recordings have a high temporal resolution (< 1 ms), its spatial resolution is limited due to volume conduction (Nunez, 1981). Volume conduction is the transmission of electrical fields from the current source in the brain through the head tissues (brain, skull and scalp) towards the scalp electrodes. Different conductivities of the tissues, especially the low conductivity of the skull, attenuate and blur the electrical potentials measured on the scalp. Consequently, maximal activity at particular electrodes on the scalp surface does not unambiguously indicate that the active sources are located in the underlying area. To find the exact source locations the source configuration in the brain has to be estimated from the potential distribution on the scalp (i.e. inverse problem). The inverse problem is, however, ill-posed (Helmholtz, 1853). A given potential distribution on the scalp can be generated by different source configurations in the brain.

Unraveling the inverse problem requires the introduction of various constraints, i.e. a priori assumptions about, e.g., the (spatially extended) volume conductor and the number and type of sources (Fender, 1987). The volume conductor (or head model) specifies how the sources in the brain produce the potentials measured on the scalp and includes information about the conductivities and shape of the volume in which the signals are generated. The simplest head model is the spherical head model. Using this model one assumes that the head consists of three concentric homogenous spherical shells, representing the brain, skull and scalp (de Munck, 1988). This model is computationally fast and easy to implement, but a strong limitation of this model is that the 'proper' head geometry is not taken into account. To improve that one may use a boundary element method (BEM) model (Fuchs *et al.*, 2002) based on the realistic geometry of the head. For this, anatomical information from brain images, obtained via MRI, are typically used to extract the surfaces for the brain, skull and scalp and these surfaces are included in the definition of the BEM model. For this model one further assumes that the tissue conductivities are uniform and isotropic (i.e. not directionally dependent). Note that because of this assumption the BEM model neglects non-uniformities, like skull holes, and anisotropies in, for example the white matter tracts in the brain. Another realistic head model, the finite element method (FEM) model, takes these factors into account (Buchner *et al.*, 1997), but this model has large computational costs and detailed information about the tissue conductivity and anisotropy is most of the times not available. The BEM model is therefore the most widely used realistic head model, because it is a compromise between the over-simplified spherical shell model and the complex FEM model.

One of the most commonly used source models to find the generating sources of SEPs is the equivalent current dipole (ECD) model (Scherg, 1990). According to this model the cortical currents can be modeled as current dipoles, which are described by their three-dimensional location, orientation and amplitude. The a priori assumption of the ECD model is that a limited number of current dipoles in the brain can explain the measured scalp potentials. To find the dipole locations the forward model has to be included. The forward model, also referred to as the leadfield, provides an estimate of the scalp potentials for a specific set of dipoles, using the electrode positions on the scalp and the selected head model. Subsequently, the modeled potential map is compared with the actual measured potential map using a least-square source estimation. This implies that the source parameters, the location, orientation and strength of each dipole, are manipulated until the squared error between the modeled and actual data is minimal. The dipole locations of the optimal solution are assumed to be the generating sources of SEP.

3 Methods & Procedures

3.1 Subjects

Young and older healthy subjects were recruited from the students and staff of the VU University and the VU University medical center (VUmc). Some healthy subjects were also recruited using recruitment letters. Patients in the chronic phase post stroke (more than 6 months after stroke) were recruited from the Department of Rehabilitation Medicine of the VUmc, Amsterdam and the Reinier de Graaf Hospital (RdGG), Delft. For these patients relevant clinical characteristics, including gender, age, location of lesion, time post stroke and degree of upper limb function were registered. The stroke patients initially experienced acute paresis of the upper limb following stroke and some patients still had a paresis in the chronic phase. Exclusion criteria were multiple strokes, other neurological disorders, head trauma, other disorders affecting the hand and arm function and severe psychiatric disorders. People with metal implants in their body were also excluded from the study, because they were not able to undergo Magnetic Resonance Imaging (MRI). All participants gave a written informed consent before participation. This study is part of the 4D-EEG project in which the relation between upper limb function and brain activity patterns is investigated (www.4deeg.eu). This longitudinal study with repeated EEG measurements aims to construct a detailed functional image of the brain in the early period post stroke. The study protocol was approved by the Medical Ethics Committee of the VU University Medical Center (Protocol: NL47079.029.14).

3.2 Procedures

Clinical assessments were first conducted to assess patients' upper limb function. SEPs were evoked and recorded using EEG. During the measurements all participants were seated in a wheelchair with the hands comfortably resting on the knees. The participant was instructed to look at a fixed point at eye height and sit as still and relaxed as possible. The neurophysiological examination took place in a survey van, which made it possible to perform the measurements at participants' homes. In addition, three-dimensional T1-weighted MR images were obtained for all subjects using a 3T MRI scanner located in the VU University Medical Center. The MR and EEG recordings were performed on different days.

3.3 Data acquisition

3.3.1 Clinical assessments

Motor function was assessed using the upper extremity section of the Fugl-Meyer Motor Assessment (FMA) (Fugl-Meyer *et al.*, 1975). The FMA measured the extent to which the patient was dependent on synergistic movements and included items dealing with movements of the shoulder, elbow, wrist and hand. Each item was scored on a 3-point ordinal scale and the scores of all items added up to a maximum score of 66 points. In addition, upper limb capacity was assessed using the Action Research Arm Test (ARAT) (Lyle, 1981). The items of the ARAT were divided into four subtests: grasp, grip, pinch and gross movement. Performance on each item was scored on a 4-point ordinal scale, with a maximum score of 57 points. The ARAT and FMA are both reliable and valid clinical measures (Duncan *et al.*, 1983; van der Lee *et al.*, 2002).

3.3.2 Neurophysiological examination

SEPs were evoked by electrical stimulation (Micromed S.p.A., version ENERGY, Italy) of the index finger of the affected hand for patients and the dominant hand for healthy controls. Two stimulating electrodes were placed 1 cm apart on the index finger with the anode distal and the cathode

proximal to the distal interphalangeal joint. The stimuli were delivered at a repetition rate between 3 and 4 Hz, with a pulse duration of 400 μ s and a stimulus intensity of twice the sensory threshold. The sensory threshold was determined for each participant independently. Starting at a low stimulus intensity, the amplitude of the electric current was increased until the subject was able to detect five of the ten applied stimuli. For patients the sensory threshold was determined at the non- or less affected upper limb.

SEPs were obtained by averaging the recordings after 1000 stimuli. Two separate blocks of 500 stimuli were performed with a short break between both blocks. Within a block the inter-stimulus interval between two successive stimuli was varied randomly, between 250 ms and 333 ms, to ensure attention of the participant.

3.3.3 EEG recordings

The cortical potentials were continuously recorded using a 64-channel EEG Refa-72 system (ANT, the Netherlands). A 64-channel EEG cap with Ag/AgCl electrodes was placed on the scalp. An external ground electrode was placed on the left mastoid process. The channels M1 and M2, which were located at the left and right mastoid, were therefore not used. The arrangement of the electrodes in the cap was in accordance with the international 10-20 system. The electrode-skin impedance was monitored at a level below 20 k Ω , using conductive gel. The signals from all channels were recorded at a sampling rate of 2048 Hz using ASA software (ANT, the Netherlands) and a common average reference was used. The onsets of the electrical stimuli were synchronized with the EEG using Matlab (R2014a, The Mathworks, Natick, MA).

Before the EEG recording the positions of the three fiducials, nasion, left and right pre-auricular points, and the electrode positions were measured using a 3D digitizer (Xensor 3D Electrode Digitizer system, ANT, The Netherlands). These data were used for source modeling and co-registration of the 62 EEG electrodes with the subject's MRI data.

3.4 Data analysis

3.4.1 Preprocessing

The EEG data were analyzed off-line using Matlab (R2014a, The Mathworks, Natick, MA) and the Fieldtrip Toolbox (Oostenveld *et al.*, 2011). For all channels an artifact caused by the stimulus was present around stimulus onset and 10 ms after stimulus onset. The stimulus artifact was therefore removed for all trials by interpolating a straight line between 1 ms pre to 3 ms post stimulus onset and between 9 ms and 13 ms post stimulus onset. A 50Hz notch filter and a 1Hz high pass filter were applied to the stimulus artifact-free data. In addition, a low-pass Savitzky-Golay smoothing filter was used (Savitzky & Golay, 1964). The Savitzky-Golay filter performs an unweighted linear least-squares fit to windows of a given size using a polynomial of a given order. The lower the polynomial order and the larger the window size, the higher the level of smoothing. In this study a window size of 21 samples and polynomial of order 4 was used.

Independent Component Analysis (ICA) was subsequently applied to the filtered, continuous data to identify and remove artifacts caused by eye blinks, eye movements and muscle activity. Independent components (ICs) mainly projecting to the frontal sites and containing large deflections characteristic for eye blinks and eye movements were removed. ICs projecting to the temporal and occipital sites and containing high amplitude, fast activity (median frequency around 60Hz) were assumed to be muscle artifacts (O'Donnell *et al.*, 1974) and were also removed.

Subsequently, the continuous recordings were segmented in time windows lasting 50 ms before to 250 ms after stimulus onset. Trials and channels assumed to be outliers, based on their variance, were removed. The variance varied widely between subjects, but at least 80% of the

trials were maintained to ensure a sufficient signal-to-noise ratio. The remaining trials were re-referenced to the common average reference and averaged to one SEP, resulting in one SEP for every subject.

3.4.2 Sensor level analysis

P50 and P100 were first identified at sensor level. For both P50 and P100 the electrode displaying the largest positive value and the electrode displaying the largest negative value were selected. The four nearest electrodes were also selected, forming two clusters of five electrodes. The mean positive amplitude and the mean negative amplitude for these five electrodes were calculated at, respectively, the maximal and the minimal peak amplitude. To determine the P50 and P100 amplitude the absolute values of the mean positive amplitude and the mean negative amplitude were summed. Latency for P50 and P100 was defined as the mean of the latency at minimal and at maximal peak amplitude. Additionally, the interpeak interval between P50 and P100 was determined for each subject separately by subtracting the latency for P50 from the latency for P100.

3.4.3 Source localization

A single ECD model was performed to locate the generating sources of P50 and P100. Because the single ECD model will only provide reliable results when the activity is focal, time segments in which only one of the sources is (primarily) active had to be selected. To select appropriate time windows for the localization of the P50 and P100 source a single equivalent moving dipole model was applied to the data in the time period from stimulus onset ($t=0$) to 250 ms after stimulus onset ($t=0.25$). The three-compartment (scalp, skull and brain) boundary element method (BEM) model (Fuchs *et al.*, 2002) was used as the head model. The BEM model was constructed from the MR images of the subject's head using Freesurfer, which is documented and freely available for download online (<http://surfer.nmr.mgh.harvard.edu/>). The used coordinate system was the Free-surfer coordinate system, which is based on the so-called RAS coordinates. This means that the x-axis points towards Right, the y-axis points towards Anterior and the z-axis points towards Superior. The origin is defined as the center of a $256 \times 256 \times 256$ isotropic 1 mm^3 volume. The source space was defined as a three dimensional grid with a grid resolution of 5 mm. For every point in time the defined source space was scanned with a single ECD and at the most optimal location a non-linear fit started. Subsequently, the goodness of fit (GOF) was determined for the resulting dipole locations. The GOF can be expressed as the percentage of explained variance. Only the dipole locations having a GOF of 70% of the maximal GOF were selected. These dipole locations were grouped into clusters using a hierarchical clustering analysis available in Matlab.

The hierarchical clustering procedure starts with a set of K dipole locations with each location in a cluster of its own. The closest pair of clusters is united into one cluster, which results in $K - 1$ clusters. It is then examined if a third location should be united with the first pair or that a new pair is formed. This can be continued until all K dipole locations are grouped into the specified number of clusters, which is determined a priori. In the present analysis five clusters were used. The Euclidean distance between dipole locations i and j was defined as:

$$d_{ij} = d(\vec{X}_i, \vec{X}_j) = \sqrt{(X_{i,x} - X_{j,x})^2 + (X_{i,y} - X_{j,y})^2 + (X_{i,z} - X_{j,z})^2} \quad (1)$$

The linkage method defines how the distance between clusters is measured. Several linkage methods were examined and results were comparable. It was eventually decided to use the Ward's method (Ward, 1963) as the linkage method. According to this method the distance between two clusters is the increase in the within-cluster sum of squares when two clusters are merged. The

within-cluster sum of squares is defined as the sum of squares of the distance between all dipole locations and the centroid of the cluster. The distance (D) when cluster A and B are merged into cluster C is defined as:

$$D = \sum_{i \in C} d(\vec{X}_i, \vec{M}_C) - \sum_{i \in A} d(\vec{X}_i, \vec{M}_A) - \sum_{i \in B} d(\vec{X}_i, \vec{M}_B) \quad (2)$$

where $\vec{M}_A, \vec{M}_B, \vec{M}_C$ is the center of respectively cluster A, B and C and i the number of points in it. In the beginning the total sum of squares is zero, because every cluster contains only one dipole location. The sum of squares will, however, increase when the clusters are merged. Ward's method tries to keep this increase as small as possible.

The clusters formed during the aforementioned procedure were evaluated over time and periods for the localization of the P50 and P100 source were selected. Different assumptions were made a priori. First, it was assumed that dipole locations belonging to the P50 source are clustered into a different cluster than the dipole locations belonging to the P100 source. Secondly, it was assumed that the dipole location is stable during the period that only the source of P50 or only the source of P100 is active. Finally, it was assumed that the P50 source can best be localized around 60 ms and the P100 source around 120 ms. Around 60 ms the activity of SI is already high, while the activity of SII is just beginning to increase. Around 120 ms SII is still active, while the SI activity is decreased (Elbert *et al.*, 1995). The two time segments best meeting these criteria were selected for the single ECD model. The source space was again defined as a three dimensional grid with a grid resolution of 5 mm and the location, orientation and strength of the ECD were again estimated within a three compartment BEM model (Fuchs *et al.*, 2002).

3.4.4 The source parameters

After estimation of the dipole positions for P50 and P100 the location and orientation were examined for both sources. To examine the location both dipole locations were first normalized to a template MRI in MNI space. The MNI coordinate system is comparable to the Freesurfer coordinate system, but the origin is different. The origin of the MNI coordinate system is the anterior commissure instead of the center of a $256 \times 256 \times 256$ isotropic 1 mm^3 volume. The difference in location between the P50 and P100 source was examined using the Euclidean distance between the normalized dipole locations (1). To verify if the P50 and P100 sources were located in, respectively, SI and SII the normalized dipole locations were compared with an anatomical atlas. The WFU Pickatlas (Version 3.0.5b, Wake Forest University, School of Medicine, NC, USA) on which the Brodmann areas (BA) are indicated was used as the anatomical atlas. BA 1, 2 and 3 correspond to SI and parts of BA 40 and 43 correspond to SII (Benarroch, 2006).

To examine the orientation of the P50 and P100 source a principal component analysis (PCA) was applied to the dipole moments in the x-, y- and z-direction. PCA is defined as an orthogonal linear transformation that transforms the original data into a new coordinate system. The principal components (PCs) are found by calculating the eigenvectors and corresponding eigenvalues of the covariance matrix of the data. The eigenvector with the largest eigenvalue, also called the first PC, is the direction of the greatest variance. This direction will become the new x-axis. The eigenvector with the second largest eigenvalue is the direction of the second greatest variance and this will become the new y-axis. The last eigenvector will become the z-axis. The first PC was considered as the orientation of the source, since the eigenvector of the first PC explains most of the variability that is present in the data. The difference in orientation between the P50 and P100 source was calculated using the dot product of the eigenvectors of the P50 and P100 source. The dot product is directly related to the cosine of the (smallest) angle between the two vectors. This

angle is constrained to be between 0 and π radians, because it is equal to the shortest great-circle distance between the two vectors.

3.5 Statistical analysis

Descriptive statistics for all data are expressed as mean \pm standard deviation and were, if possible, compared between groups. The differences in latency and amplitude of the P50 and P100 SEP-component and the differences in interpeak interval between young healthy subjects, older healthy subjects and patients were examined with a one-way between subjects ANOVA. Partial eta-squared (η_p^2) values were calculated to determine the effect size. To identify where specific differences occurred between groups independent sample t-tests were performed using Bonferroni adjusted alpha levels of .0167 per test (.05/3). The assumption of normality was checked by visual inspection of the Q-Q plots and the box plot of the data within groups. A Shapiro-Wilks test was also performed on the data within the groups. The assumption of homogeneity of variance was checked using the Levene's test. When the assumptions of normality was violated the non-parametric Kruskal-Wallis test was used.

The difference in location and orientation between the P50 and P100 source were both transformed before statistical tests were applied. The difference in location was biased to positive values and was transformed using a logarithmic transformation. The difference in orientation was constrained to be between 0 and π . The data were therefore first divided by π , 0.5 was subtracted and the data were multiplied by 2 to convert the data to a range between -1 and 1. The Fisher z-transformation was then applied to the data, which is the inverse hyperbolic tangent of the data (Fisher, 1921). Subsequently, the difference in location and orientation between P50 and P100 was compared between groups using a one-way between subjects ANOVA. Level of statistical significance was defined as $p < .05$. For the statistical analysis the software package IBM SPSS Statistics for Windows was used (Version 22.0, IBM Corp., Armonk, NY, USA).

4 Results

4.1 Demographic data and clinical characteristics

Ten young healthy subjects (5 women, 5 men; mean = 28.5 ± 5.4 years; 9 right-handed), four older healthy subjects (3 men, 1 women; mean = 52.0 ± 5.4 years; 4 right-handed) and six chronic stroke patients (5 men, 1 women; mean = 63.2 ± 8.4 years) were included in this study. Clinical characteristics and the scores for the ARAT and FMA are summarized in table 1 for all patients. Patient 4 and 5 were excluded from further analysis, because clear dipolar distributions around 50 ms and 100 ms were lacking and no visible SEP components could be detected. These subjects also indicated during the measurements that they were not able to detect the stimuli applied to their paretic hand. In addition, these patients had the lowest scores for the ARAT and FMA (see table 1). Consequently, only four patients (4 men, 0 women; mean = 64.8 ± 9.1 years) were included in the remainder of the analysis. Age was significantly higher in the group of older healthy subjects than in the group of young healthy subjects and was also significantly higher in patients when compared to older healthy subjects. The women/men ratio was higher in the group of young healthy subjects, when compared to the group of older healthy subjects and patients.

Table 1. Patient characteristics and the ARAT and FMA scores.

Patient number	Gender	Age (year)	Time poststroke	Affected body side	ARAT	FMA
1	Male	64	7 years	Left	5/57	13/66
2	Male	63	4 years	Right	54/57	39/66
3	Male	77	8 mth	Left	51/57	62/66
4	Female	66	18 years	Right	3/57	9/66
5	Male	54	1.75 years	Left	4/57	8/66
6	Male	55	6 years	Left	57/57	58/66

ARAT: Action Research Arm Test, FMA: Fugl-Meyer Motor Assessment

4.2 Amplitude and post-stimulus latency

The stimulus intensity was, on average, 2.2 ± 0.6 mA for young healthy subjects, 3.0 ± 0.6 mA for older healthy subjects and 3.0 ± 0.8 mA for chronic stroke patients. Due to a change in the stimulation protocol during the experiment only one block of 500 stimuli was available for one young healthy subject, for one older healthy subject and for two patients. During the preprocessing of the EEG data 99 ± 48 trials, 3 ± 3 channels and 21 ± 7 ICs were removed for each subject.

The mean latencies for P50 and P100 and the interpeak interval for all groups are presented in figure 2. For young healthy subjects the P50 and P100 latency was, respectively, 49.6 ± 9.2 ms and 95.2 ± 14.8 ms, for older healthy subjects 53.5 ± 5.5 ms and 112.5 ± 6.4 ms and for chronic stroke patients 54.5 ± 11.1 ms and 105.4 ± 14.8 ms. Latency for both P50 ($F(2,15)=0.53$, $p = .601$, $\eta_p^2 = .07$) and P100 ($F(2,15)=2.57$, $p = .110$, $\eta_p^2 = .26$) and the interpeak interval between P50 and P100 did not significantly differ between groups ($F(2,15)=1.53$, $p = .249$, $\eta_p^2 = .17$).

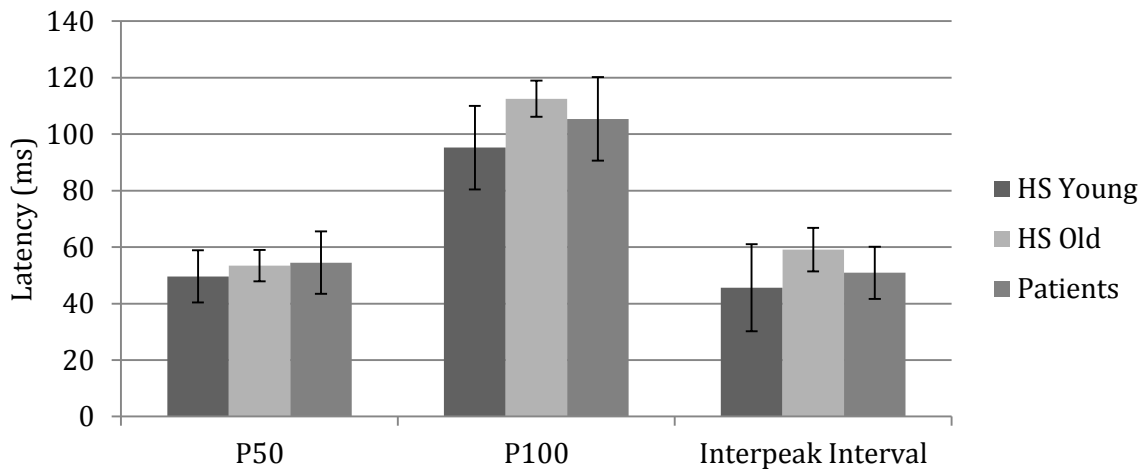


Figure 2. Post-stimulus latency for P50 and P100 and the interpeak interval between P50 and P100 for young healthy subjects (HS Young), older healthy subjects (HS Old) and chronic stroke patients (Patients). Displayed are the mean values in milliseconds. Error bars indicate the standard deviations.

The mean amplitudes for P50 and P100 for all groups are presented in figure 3. The group effect for the P50 amplitude almost approached significance ($F(2,15)=3.48$, $p = .057$, $\eta_p^2 = .32$) and also for the P100 amplitude a weak trend toward significance was present ($F(2,15)=2.64$, $p = .104$, $\eta_p^2 = .26$). For the P50 amplitude the biggest difference was found between young and older healthy subjects. The P100 amplitude was bigger for young healthy subjects when compared to both older healthy subjects and chronic stroke patients. However, this group effect did not reach significance, which may be due to the small sample sizes and the variations within groups.

For patients the individual values for the amplitude, latency and interpeak interval are also presented in table 2. As can be seen from this table patient 6 had the biggest and patient 1 the

smallest amplitude for P50. These patients also had the highest and lowest scores for the ARAT and FMA (see table 1). This was, however, not the case for the P100 amplitude and the post-stimulus latency for P50 and P100.

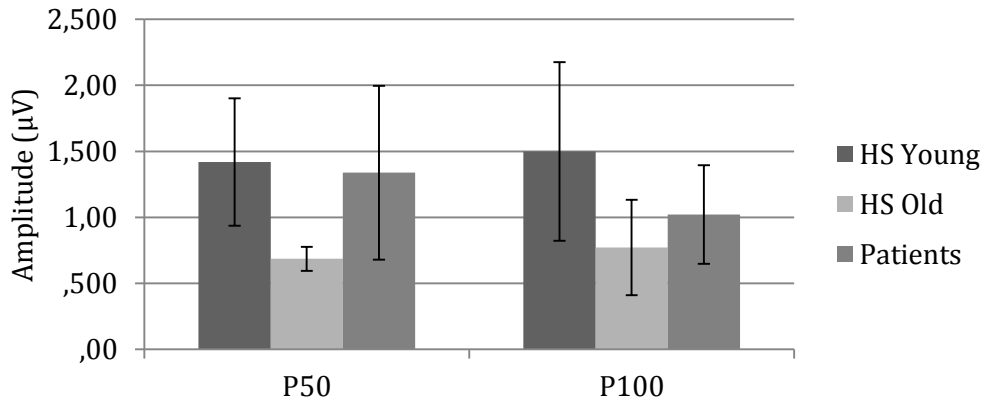


Figure 3. Amplitude for P50 and P100 for young healthy subjects (HS Young), older healthy subjects (HS Old) and chronic stroke patients (Patients). Displayed are the mean values in microvolts. Error bars indicate the standard deviations.

Table 2. P50 and P100 amplitude and latency for patients.

Patient number	P50 latency	P50 amplitude	P100 latency	P100 amplitude	Interpeak interval
1	64.5	0.86	107.2	1.05	50.5
2	50.7	0.93	112.5	0.49	62.2
3	40.5	1.27	84.2	1.24	42.4
6	62.3	2.28	117.7	1.31	60.1

Latency and interpeak interval are expressed in milliseconds and the amplitude in microvolts.

4.3 Source localization

4.3.1 Young healthy subjects

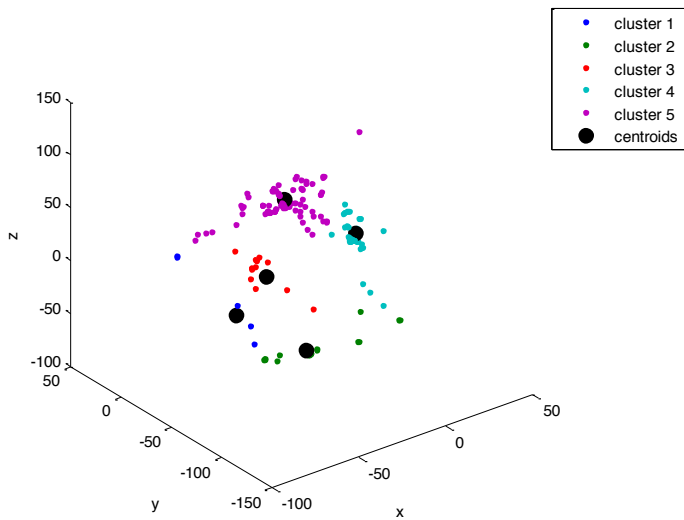
On average, the time period from 39.7 ± 8.6 ms to 52.9 ± 9.6 ms and the time period from 82.2 ± 14.7 ms to 97.4 ± 22.0 ms were selected for the localization of, respectively, the P50 and P100 source in young healthy subjects. This is earlier than the time periods suggested by Elbert and colleagues (1995). According to this study the best time to locate SI is around 60 ms and SII around 120 ms. However, the exact latencies are dependent on the inter-stimulus intervals and the side of stimulation. In the study of Elbert and colleagues (1995) median nerve stimulation was used instead of finger stimulation and the inter-stimulus-interval was almost four times longer than the inter-stimulus interval used in this study. Although it was assumed that the dipole locations belonging to the P50 and P100 source were clustered into different clusters, for seven subjects the dipole locations fell within the same cluster. For these subjects the number of clusters was increased to maximal 10 clusters. For three subjects, however, the cluster containing the dipole locations for both P50 and P100 remained intact and the dipole locations for P50 and P100 were only separated by time.

Figure 4 provides the results of the hierarchical clustering approach for young healthy subject 1. For this subject the maximal GOF in the time period from stimulus onset to 250 ms after stimulation was 0.697. Thus, all dipole locations having a GOF higher than 0.488 were selected for the hierarchical clustering approach. Most dipole locations fell within cluster 4 and 5. The dipoles in clusters 1, 2 and 3 were located in the occipital part of the brain and were therefore excluded. Because cluster 5 is mainly active after 150 ms it was assumed that the dipole locations belonging to P50 and P100 both fell within cluster 4. The number of clusters was increased to 10 clusters to

examine whether cluster 4 would be separated into different clusters when more clusters are used. Cluster 4 remained, however, intact. The time period in which cluster 4 was first active, from 28 ms to 59 ms, was therefore selected for the localization of the P50 source and the time period in which cluster 4 was active for the second time, from 73 ms to 85 ms, for the localization of the P100 source.

Unfortunately, it was not clear for all subjects which clusters and time segments had to be selected for source localization based on the hierarchical clustering procedure. For three subjects more than two clusters and/or time segments met the pre-determined criteria and the selection of time windows for source localization was therefore quite arbitrary and subjective. For one subject none of the clusters did meet the predetermined criteria properly. For these four subjects the latencies for P50 and P100, which were found at sensor level, were also taken into consideration during the selection of clusters.

A



B

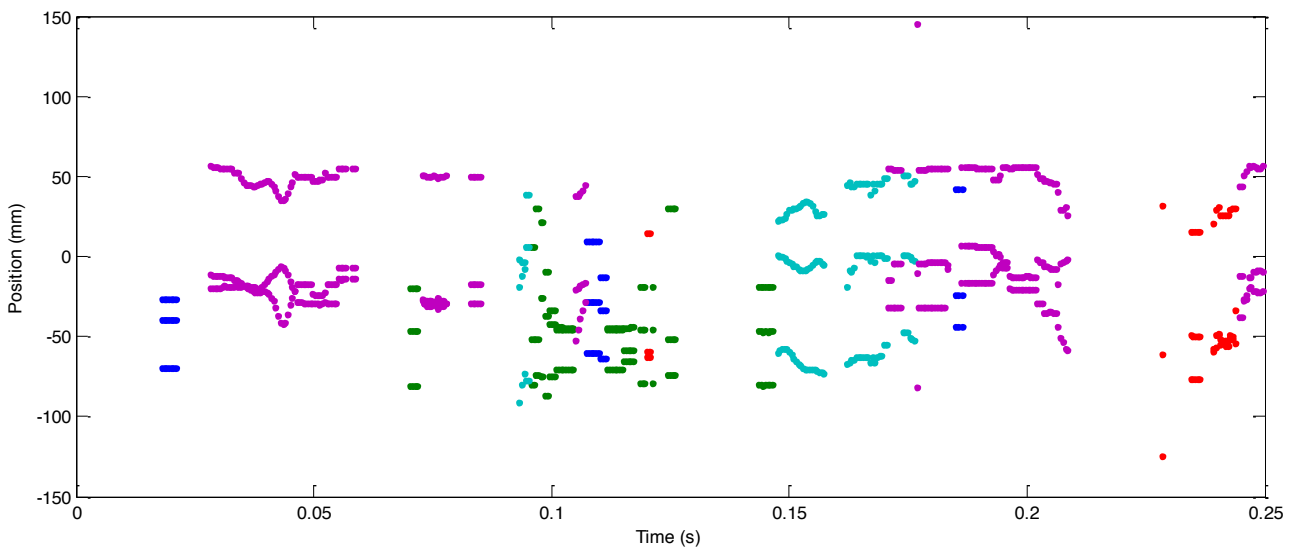


Figure 4. Dipole locations of young healthy subject 1 grouped into five clusters (A) and plotted over time (B). Time is expressed in seconds and position in millimeters.

The normalized location and the orientation of the P50 and P100 source for young healthy subject 1 can be found in figure 5. As can be seen from figure 5 the dipole for P50 is located somewhat more lateral and posterior to the dipole for P100. Both sources have an inferior-superior current direction. Figure 6 illustrates the time series of both sources when the analysis was extended to the whole time period using the positions of the dipoles for P50 and P100 as the locations of interest. For both sources the response can be found in the inferior-superior direction (z -axis). The maximal activity for the P50 source is around 37 ms and for the P100 source around 74 ms. This is in agreement with the latencies found at sensor level, where P50 was found at 40 ms and P100 at 73 ms. However, when the dipole locations for P50 and P100 are compared with the anatomical atlas the dipole for P50 seemed to be located in BA 6 and the dipole for P100 in BA 1, 3 and 6. BA 6 corresponds to the premotor cortex and supplementary motor cortex, which are located anterior to SI. BA 1 and 3 corresponds to SI.

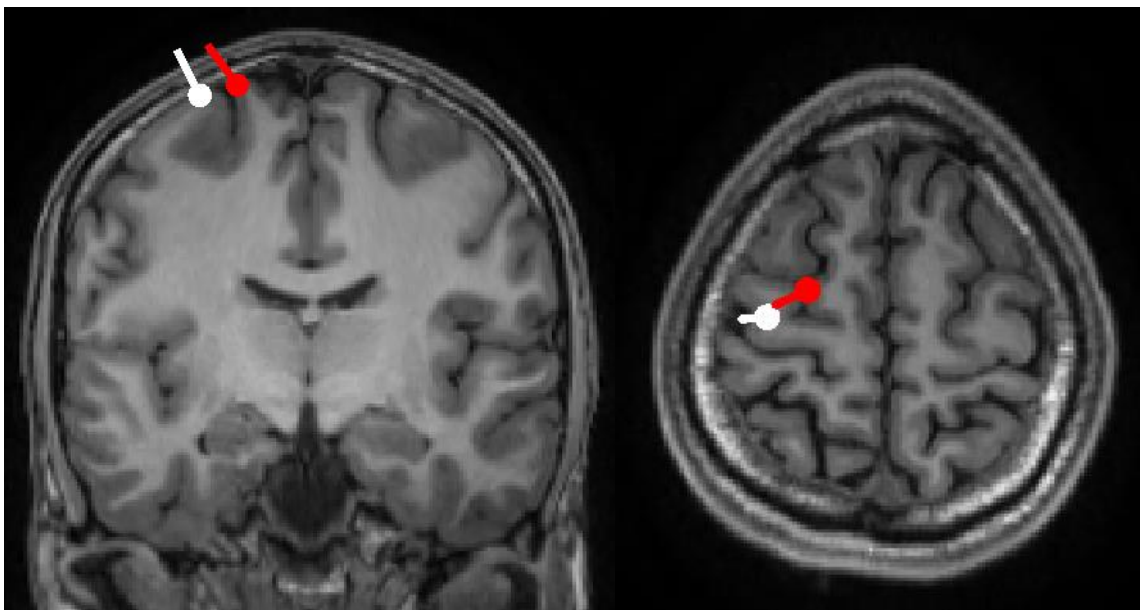


Figure 5. The normalized anatomic location of the generator sources of P50 (red) and P100 (white) onto a template MRI for young healthy subject 1. The normalized location and orientation of the sources are indicated by the circle and the bar, respectively. This subject was stimulated on the right side.

The normalized dipole locations for P50 and P100 and the corresponding BA for the other young healthy subjects are presented in table 3. For all subjects different locations for the P50 and P100 source were found. For young healthy subject 2 the dipole for P50 is located in SI (BA 1, 2, 3). For the other subjects the dipole for P50 is located anterior (BA 4, 6) or posterior (BA 5, 7, 39, 40) to SI. BA 4 corresponds to the primary motor cortex. BA 5, 7, 39 and 40 all correspond to the posterior parietal cortex. For subject 8 no BA could be defined, because the dipole was located just outside the brain, in the scalp. This is probably due to an error in the construction of the head model or the co-registration of the electrodes with the head model. The dipole locations for P100 were also not located in SII for most subjects. Only for subject 9 the dipole for P100 is located in BA 40, which corresponds to SII. For the other subjects the dipole for P100 is located in the posterior parietal cortex (BA 7), in SI (BA 1, 2, 3) or anterior to SI (BA 4, 6). For subject 9 the dipole for P100 is located in the frontal eye fields (BA 8), which is probably due to noise.

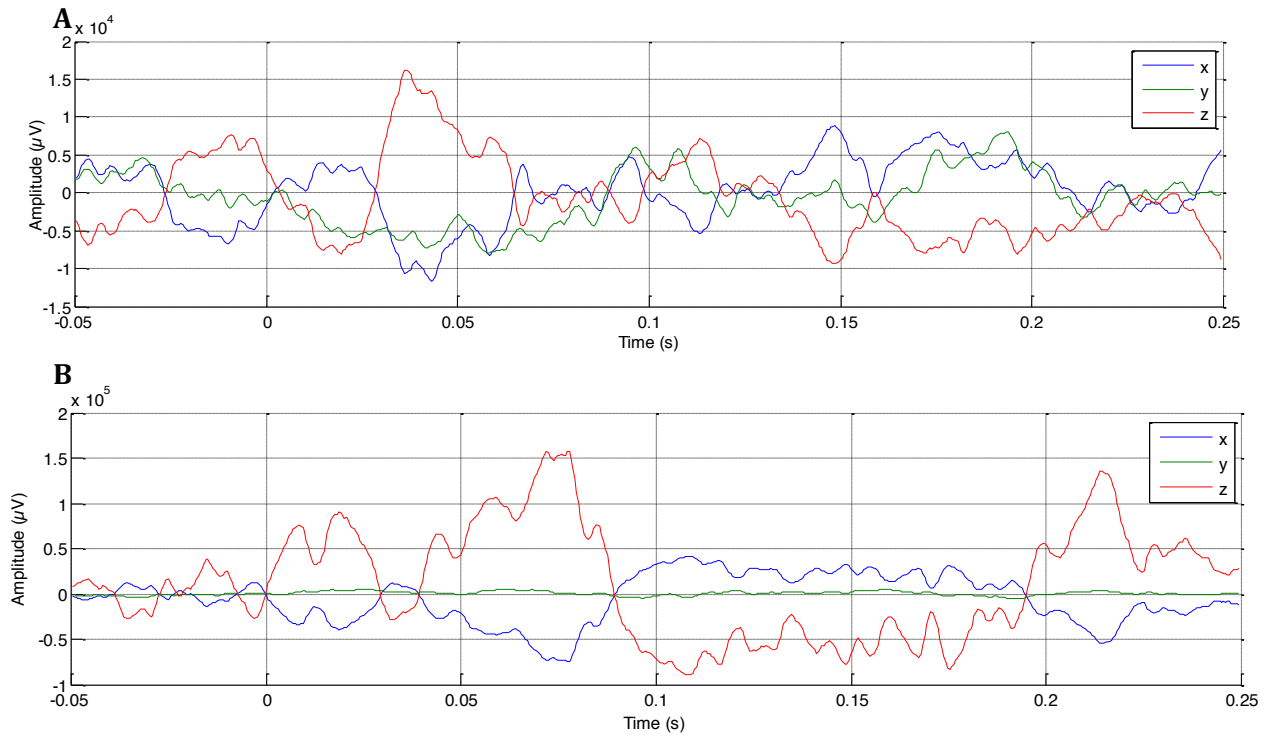


Figure 6. The dipole moments in x, y and z direction for the dipole found for P50 (A) and for P100 (B) for young healthy subject 1. Time is expressed in seconds and the dipole moment in microvolts.

Table 3. The normalized dipole locations for P50 and P100 and corresponding Brodmann Areas (BA) for all ten young healthy subjects (HS Young).

HS Young	P50				P100				ΔL	ΔO
	x	y	z	BA	x	y	z	BA		
1	-20,84	-11,57	84,48	6	-31,53	-18,70	81,55	1,3,6	13,18	0,22
2	-39,85	-25,62	77,75	1,2,3	-29,26	-13,34	80,50	6	16,44	0,14
3	-18,64	-37,49	87,37	5,7	-23,88	-48,21	80,65	7	13,69	1,75
4	-42,06	-2,16	61,58	4,6	-32,38	-53,35	54,20	7	52,62	2,84
5	-21,20	-12,77	87,31	6	-17,56	-32,14	85,94	1,2,5	19,75	0,23
6	-37,00	-34,47	53,72	40	-26,75	-48,72	67,75	7	22,48	0,22
7	-29,38	3,32	76,26	6	-24,15	25,99	43,07	8	40,54	1,57
8	-45,02	-19,61	85,66	Nan	-36,04	-32,98	78,74	2	17,53	1,92
9	49,35	-2,82	64,73	6	70,94	-25,72	36,77	40	42,10	1,44
10	-51,76	-72,21	46,90	39	-45,88	-7,54	72,17	3,4,6	69,68	0,39

The dipole locations are expressed in millimeter and in MNI space. The x-axis points towards right, the y-axis points towards anterior and the z-axis points towards superior. Subject 9 is left-handed. ΔL = difference in location between the P50 and P100 source. ΔO = difference in orientation between the P50 and P100 source.

4.3.2 Older healthy subjects

On average, the time period from 44.1 ± 6.9 ms to 54.0 ± 10.4 ms and the time period from 91.1 ± 11.1 ms to 100.5 ± 10.4 ms were selected for the localization of, respectively, the P50 and P100 source. For older healthy subject 2 the dipole locations for P50 and P100 were clearly separated in two different clusters and it was clear which time segments had to be selected. The dipole locations for P50 and P100 fell within the same cluster for the other three subjects. For subject 1 it was still clear which time segments had to be selected, but for subject 3 multiple clusters met the predetermined criteria. For subject 4 no periods in which the dipole location was stable could be found. The selection of clusters was for subject 3 and 4 therefore also based on the latencies found at sensor level.

The normalized dipole locations for P50 and P100 and the corresponding BA for all older healthy subjects are presented in table 4. For all older healthy subjects different source locations were found for the sources of P50 and P100. As expected, for subject 3 the P50 response was located in SI and the P100 response in SII. For this subject the normalized location and the orientation of both sources are presented in figure 7. As can be seen from this figure both ECDs are pointed in the superior-inferior direction. For subject 2 the dipole for P50 is located in SI, but the dipole for P100 is located in the posterior parietal cortex. For subject 1 both dipoles are located anterior to SI (BA 6) and for subject 4 both dipoles are located in and around SII (BA 40).

Table 4. The normalized dipole locations for P50 and P100 and corresponding Brodmann Areas (BA) for all older healthy subjects (HS Old).

HS Old	P50				P100				ΔL	ΔO
	x	y	z	BA	x	y	z	BA		
1	-40.80	0.83	66.60	6	-20.72	8.82	75.22	6	23,27	2,85
2	-43.61	-36.55	75.18	2,5	-29.81	-36.60	77.89	5,7	14,06	0,98
3	-51.03	-6.28	63.03	3,4,6	-42.56	-47.64	65.65	40	42,30	1,71
4	-64.53	-37.40	53.30	40	-53.55	-27.98	65.03	2,40	18,62	2,63

The dipole locations are expressed in millimeter and in MNI space. The x-axis points towards right, the y-axis points towards anterior and the z-axis points towards superior. ΔL = difference in location between the P50 and P100 source. ΔO = difference in orientation between the P50 and P100 source.

4.3.3 Chronic stroke patients

For the group of patients the time period from 46.4 ± 15.3 ms to 56.4 ± 22.7 ms and the time period from 104.2 ± 17.1 ms to 112.1 ± 19.0 ms were selected for the localization of the sources of, respectively, P50 and P100. For patient 1 and 4 it was clear which clusters and time segments had to be selected for source localization. For patient 2 and 3 no periods in which the dipole location was stable could be found. For these patients the dipolar distribution found at sensor level was also less present when compared to patient 1 and 4. In addition, the dipole locations having the highest GOF were located around the eyes or at the back of the head. The latencies for P50 and P100 at sensor level were therefore also taken into consideration for the selection of the most appropriate clusters.

The normalized location and orientation of the P50 and P100 source for patient 4 are presented in figure 8. Both dipoles were located in the posterior parietal cortex and pointed in the superior-inferior direction. The normalized dipole locations for P50 and P100 and the corresponding BA for all patients are presented in table 5. For all patients different locations were

found for the sources of P50 and P100. However, for all patients the dipole for P50 was not located in SI. The dipole was located anterior to SI for patient 1 and 3 and posterior to SI for patient 2 and 4. Although patient 2 is stimulated on the right side the dipole for P50 is just located in the right hemisphere, indicated by a small, positive x-value. The dipole for P100 is, however, as expected located in SII for this patient. For patient 3 and 4 the dipole for P100 is located in the posterior parietal cortex and for patient 1 in the motor area.

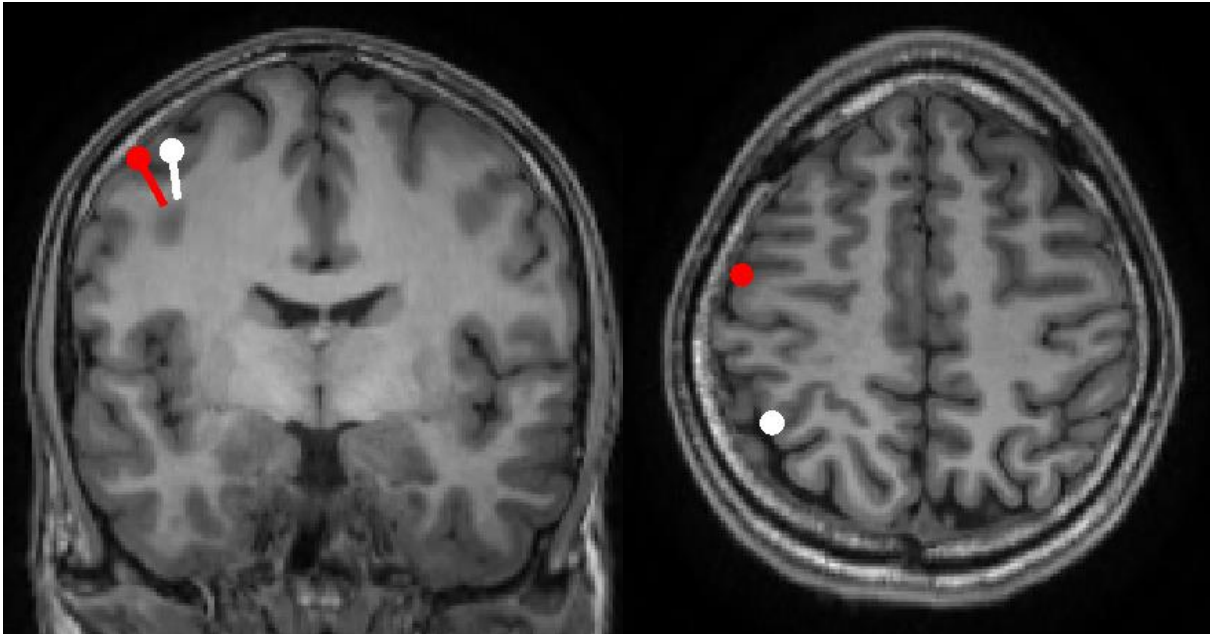


Figure 7. The normalized anatomic location of the generator sources of P50 (red) and P100 (white) onto a template MRI for older healthy subject 3. The normalized location and orientation of the sources are indicated by the circle and the bar, respectively. This subject was stimulated on the right side.

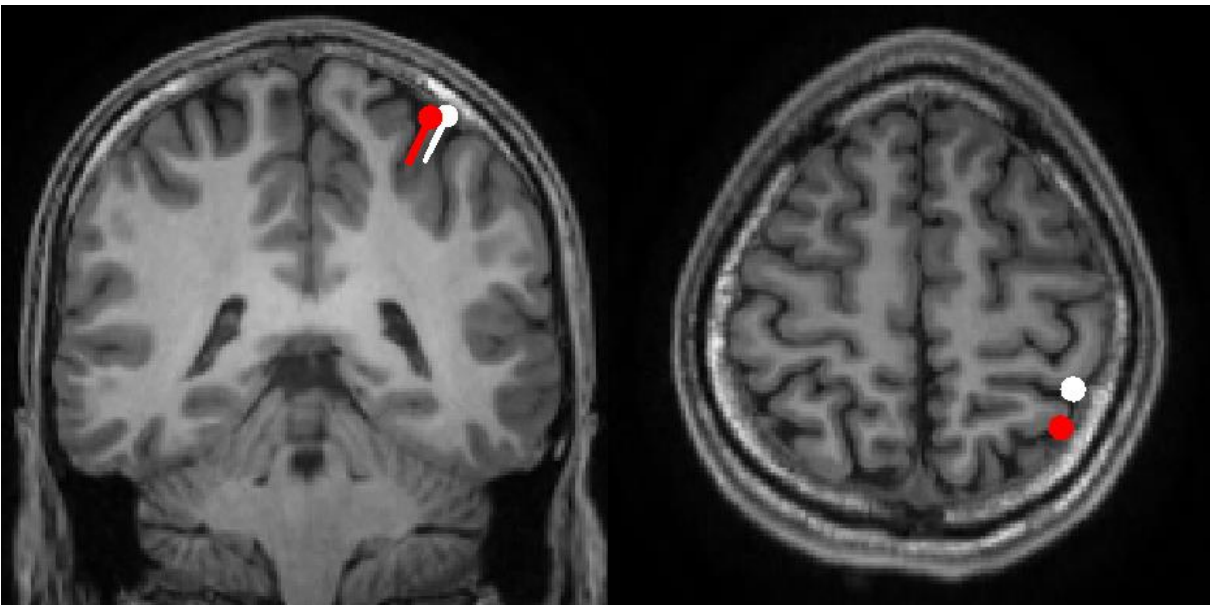


Figure 8. The normalized anatomic location of the generator sources of P50 (red) and P100 (white) onto a template MRI for patient 4. The normalized location and orientation of the sources are indicated by the circle and the bar, respectively. This subject was stimulated on the left side.

Table 5. The normalized dipole locations for P50 and P100 and corresponding Brodmann Areas (BA) for all patients.

Patient	P50				P100				ΔL	ΔO
	x	y	z	BA	x	y	z	BA		
1	36,92	8,99	70,53	6	37,45	10,21	69,19	6	1,88	0,56
2	7,08	-51,68	87,59	7	-62,08	-28,81	54,29	40	80,10	1,81
3	7,53	-55,70	79,54	4,6	43,37	-16,94	72,23	7	53,30	0,55
4	37,65	-52,95	79,54	7	40,90	-42,67	73,09	5,7	10,79	0,16

The dipole locations are expressed in millimeter and in MNI space. The x-axis points towards right, the y-axis points towards anterior and the z-axis points towards superior. ΔL = difference in location between the P50 and P100 source. ΔO = difference in orientation between the P50 and P100 source.

4.4 Difference in location and orientation

The mean difference in the normalized location between the P50 and P100 source is for young healthy subjects 30.80 ± 19.40 mm, for older healthy subjects 24.56 ± 12.41 mm and for patients 36.52 ± 36.71 mm. After the logarithmic transformation the data was normally distributed, but the assumption of homogeneity of variances was violated. The Welch test was therefore performed. No differences were found for the P50-P100 difference in location between young healthy subjects, older healthy subjects and patients ($F(2,15)=0.182$, $p = .838$, $\eta_p^2 = .038$).

To examine the orientation of the sources a PCA was first applied to the dipole moments of P50 and P100. On average, the first PC explained for P50 95.7 ± 6.6 % and for P100 96.7 ± 4.2 % of the total variance that was present in the data. The mean difference in orientation between the P50 and P100 source is for young healthy subjects 1.08 ± 0.95 radians, for older healthy subjects 2.04 ± 0.86 radians and for patients 0.77 ± 0.72 radians. The data was normally distributed after the Fisher z-transformation (Fisher, 1921) and the groups had similar variance. Like the location, no differences were found for the difference in orientation between groups ($F(2,15)=2.288$, $p = .136$, $\eta_p^2 = .234$).

The difference in location and orientation for all subjects are presented in the last two columns of tables 3, 4 and 5. As can be seen from this tables the difference in location and orientation varies widely within groups, especially for patients. For patient 2, for example, the Euclidean distance between the P50 and P100 source is 80.10 mm, while the difference is only 1.88 mm for patient 1.

5 Discussion

This study aimed to locate and separate the sources of the P50 and P100 SEP-component after electrical finger stimulation in healthy subjects and in chronic stroke patients. Subsequently, the difference in location and orientation between the P50 and P100 source was examined and compared between groups. The difference in location and orientation between the source of P50 and P100 was expected to be smaller in stroke patients than in healthy subjects, due to reorganization of the somatosensory areas (Pons et al., 1988; Rossini *et al.*, 2001) and a possible take-over of function by one of the sources (Simoes *et al.*, 2001). Furthermore, P50 and P100 were expected to be located in SI and SII, making them excellent candidates for predicting upper limb recovery post stroke.

In contrast to previous studies no differences in the latency and amplitude of the SEPs were found between healthy subjects and chronic stroke patients, when the SEP-components were examined at sensor level (Al-Rawi *et al.*, 2009; Roosink *et al.*, 2011; Yuya *et al.*, 1996). These studies

found longer latencies and smaller amplitudes in patients. Nevertheless, there was a trend towards significance for both the P50 and P100 amplitude. Young healthy subjects showed increased amplitudes for P50 and P100 when compared to older healthy subjects and patients. Since the differences were also present between the group of young and the group of older healthy subjects the differences may not be the result of the lesion, but may be explained by other effects, like age. In addition, the group sizes were small and relatively large variations were present within groups.

For two patients no SEPs could be detected. These two patients also had the lowest scores for the ARAT and FMA, which is in agreement with previous studies investigating the predictive value of SEPs in (sub-) acute stroke patients (Al-Rawi *et al.*, 2009; Feys *et al.*, 2000; Hendricks *et al.*, 1994; Hendricks *et al.*, 1997; Keren *et al.*, 1993). According to these studies the absence of cortical SEPs is related to poor upper limb recovery. In addition, bigger P50 amplitudes were found in patients with a more improved upper limb function, which is also reported earlier in (sub-) acute stroke patients (Al-Rawi *et al.*, 2009; Keren *et al.*, 1993). However, because only four patients were included in the analysis we were not able to correlate the amplitudes and latencies for P50 and P100 with upper limb function.

To locate the generating sources of P50 and P100 a single equivalent moving dipole model was applied to the whole time period and a hierarchical clustering approach was used to separate the dipole locations belonging to P50 and P100. A single ECD model was subsequently applied to the two time periods in which the selected clusters were active. For half of the group of young healthy subjects, two older healthy subjects and two patients the hierarchical clustering approach resulted in clear clusters for the sources of P50 and P100. For the other subjects the latencies for P50 and P100 found at sensor level were also taken into account during the selection of clusters. The present study was eventually able to reveal two subject-specific dipolar sources for P50 and P100 for all subjects. In contrast to the expectation, no differences were found when the difference in location and orientation between the P50 and P100 source was compared between healthy subjects and patients. Furthermore, the P50 and P100 sources were not consistently located in, respectively, SI and SII. For most subjects the sources were located in the motor area (primary motor cortex, premotor cortex or supplementary motor cortex) or the posterior parietal cortex instead of SI and SII.

According to previous research the Euclidean distance between SI and SII in response to tactile stimuli is 39.82 mm in healthy subjects (Ploner *et al.*, 2000). The average difference in location between the P50 and P100 source found in this study was smaller for both healthy subjects and patients. However, since this study was not able to locate the P50 and P100 source in, respectively, SI and SII it is difficult to compare the observed differences with this value. Besides, the difference in location between the P50 and P100 source varied widely within groups, especially in the group of patients. For two patients a smaller difference in location between the P50 and P100 source was found, when the difference was compared with the average difference found in healthy subjects. This smaller difference could be caused by (a partial) take-over of function by one of the areas, as was hypothesized. For the other two patients, however, a larger difference in location was found compared to healthy subjects. The larger difference may be caused by over-activation of the unaffected hemisphere. For these patients the P50 source was almost located in the middle of the brain, indicated by a small x-value. When in addition to the contralateral (affected) hemisphere the ipsilateral (unaffected) hemisphere is activated within 50 ms after stimulation the dipole will be located in the middle of both sources. This was not the case for the P100 source, which makes the difference in location between both sources larger instead of smaller. Contribution of SI in the unaffected hemisphere after stroke is reported by previous studies and may contribute

to somatosensory recovery (Jang, 2011; Rossini *et al.*, 2001). Activation of the unaffected hemisphere is suggested to be the result of transcallosal disinhibition. Due to a lack of inhibitory activity from the affected to the unaffected hemisphere the excitability of the unaffected hemisphere can increase (Andrews *et al.*, 1993).

It was not possible to compare the difference in orientation between the P50 and P100 source with earlier studies. According to previous research SI is pointed in the anterior-posterior direction and SII in the inferior-superior direction (Forss & Jousmäki, 1998; Mima *et al.*, 1998), but as far as we know the difference in orientation between SI and SII was never calculated before using the dot product of the first eigenvectors of SI and SII. In addition, as with location, it is difficult to compare the orientation of the P50 and P100 source with these studies, since the sources found in this study were not located in SI and SII.

Different factors may explain why the sources for P50 and P100 were not consistently located in, respectively, SI and SII. In addition, some important remarks should be made with respect to the used analysis and methods. First of all, the used hierarchical clustering approach was not able to separate the dipole locations belonging to P50 and P100 for all subjects. For these subjects the dipole locations were only separated by time. Furthermore, for a number of subjects it was not clear which clusters had to be selected, because either multiple clusters or no clusters fully met the predetermined criteria. A possibility to improve the clustering procedure could be to include the factor time in the hierarchical clustering approach. When the formation of clusters is not only dependent on the Euclidean distance between dipole locations, but also on the time period between dipoles, the separation of P50 and 100 locations into different clusters might improve. This may lead to a more accurate selection of time segments for source localization. However, the factor time is not implemented in the hierarchical clustering analysis available in Matlab and the function should first be adapted.

A second remark that should be made with regard to the analysis is that we were not able to automatically co-register the 62 EEG electrodes with the subject's MRI using the recorded positions of the fiducials. A script for the co-registration of the electrode positions with the subject's MRI is available in the Fieldtrip Toolbox, but this script does not work properly. It was therefore necessary to align the electrodes interactively with the subject's MRI, which is a time consuming process and much less accurate. When the electrodes are interactively aligned the electrode locations may be shifted a few millimeters or possibly even a centimeter to the front, back, left or right. When the electrodes are not correctly aligned to the head model the sources will not be located properly. This may explain why for most subjects the sources of P50 and P100 were located anterior or posterior to SI and SII.

Thirdly, the GOF of the dipole locations found using a single equivalent moving dipole model was in general low and never explained more than 80% of the field variance. One of the explanations could be that too much noise was still present in the data after preprocessing. Especially the signals of the electrodes placed at the back and at the side of the head contained a lot of noise. For some participants the EEG cap was not properly aligned to the back of the head, resulting in higher impedances at the back. The EEG signals may also be contaminated by muscle activity in the shoulders and neck. For some participants it was difficult to fully relax their shoulders and neck during the measurements. Furthermore, a large artifact caused by the applied stimulus was present immediately and 10 ms after stimulation. To minimize the stimulus artifact it is suggested to use a ground electrode placed on the stimulated limb close to the stimulation site instead of a ground electrode placed on the head (Cruccu *et al.*, 2008; Mauguière *et al.*, 1999).

A second possibility could be that the stimulation frequency used in this study was too high or the stimulus intensity too low. For the clinical use of SEPs a stimulation rate between 3 to 5 Hz is

recommended (Cruccu *et al.*, 2008). However, this applies in particular for the early cortical SEPs. The amplitude of the late SEP components can be reduced at rates over 3 Hz (Mauguière *et al.*, 1999). Forss and colleagues (1994) even found that the SII response was smaller when the stimuli were applied with an inter stimulus interval of 1 second, when compared to inter stimulus intervals of 3 and 5 seconds. In the present study, however, a stimulus frequency between 3 and 4 Hz was used. To examine both the SI and SII response properly a lower stimulus frequency may be more suitable. The stimulus intensity was set at twice the sensory threshold, which is recommended and in general high enough to get adequate SEPs (Cruccu *et al.*, 2008). For patients the sensory threshold was determined at the non- or less affected upper limb. However, the sensory threshold might be higher at the affected upper limb. The two patients without visible SEPs may have felt the applied stimuli when the sensory threshold was determined at the affected upper limb. Furthermore, stimulation of the median nerve instead of the index finger might also have resulted in visible SEPs for these patients. Median nerve stimulation results in a larger SEP response and the different SEP-components are better defined (Calmes & Cracco, 1971). The study of Rossini and colleagues 2001 used median nerve stimulation in addition to finger stimulation, because cerebral responses to finger stimulation are sometimes missing, even in healthy controls. In order to obtain an adequate SEP response in as many patients as possible it may be better to use stimulation of the median nerve. It is therefore decided to use median nerve stimulation in the longitudinal study of the 4D-EEG project.

A final explanation for the low GOF could be that the data cannot be explained by only a single ECD. More dipoles may be necessary to adequately explain the data. In response to electrical stimulation SI and SII are both activated in the first 100 ms and their activities overlap in time. According to a study of Karhu and Tesche (1999) SI and SII are even simultaneously activated after median nerve stimulation instead of in series. In addition, SII in the ipsilateral hemisphere is activated shortly after activation of the contralateral hemisphere (Inui *et al.*, 2004). It is therefore difficult, and maybe impossible, to find time segments in which only one source is active. This is, however, a prerequisite for the single ECD model. Furthermore, other sources, than contralateral SI and contra- and ipsilateral SII, may be activated in the first 100 ms after stimulation of the index finger. Finger stimulation is assumed to only evoke a somatosensory response, but SI has direct projections to M1 (Jones *et al.*, 1978). The motor areas may therefore be activated in response to activation of SI. Forss and colleagues (1994) also found that an extra source in the posterior parietal cortex is active in the period from 70 to 110 ms after stimulation of the median nerve. The additional activation of these two areas may also explain why for a number of subjects the P50 and P100 source were located in the motor area or in the posterior parietal cortex instead of SI and SII. Because of the possible activation of additional sources, it is worth to consider the use of a multiple-dipole model instead of a single ECD model. An example of a multi-dipole localization procedure that could be used is the Multiple Signal Classification (MUSIC) method (Mosher *et al.*, 1992). The advantage of the MUSIC method is that the number of active sources does not have to be identified a priori. According to the study of Elbert and colleagues (1995) the MUSIC procedure is able to separate the overlapping activities of SI and SII. However, a multiple-dipole model will also introduce more parameters, which increases the risk of overfitting the data, in particular when a lot of noise is present.

This study did not correlate the difference in location and orientation between the P50 and P100 source with upper limb function, because only four patients were included in the analysis. We are therefore not able to say anything about the predictive value of the examined source parameters. Also, since the sources of P50 and P100 were not located in, respectively, SI and SII the predictive value of these sources for upper limb recovery is unclear. It is therefore necessary to

investigate the predictive value of the subject-specific P50 and P100 sources further in the longitudinal study of the 4D-EEG project. In this study the subject-specific P50 and P100 sources can be examined over time during recovery and possible changes can be correlated with upper limb function. Furthermore, when the above mentioned adjustments are made the longitudinal study may be able to locate P50 and P100 in, respectively, SI and SII.

In addition to the location and orientation of the P50 and P100 source, it would be interesting to examine the source strength in the longitudinal study. This variable was not taken into account in the present study, because it is difficult to compare source strength between subjects. In the longitudinal study, however, the relative changes in source strength within a subject and its relation to upper limb recovery can be studied. Activation of the healthy hemisphere in stroke patients was also not taken into account in the present study. However, it would be interesting to examine activation of the healthy hemisphere after stimulation of the affected upper limb as well as after stimulation of the non- or less affected upper limb. After stimulation of the affected upper limb it can be examined whether compensatory mechanisms take place in the healthy hemisphere as a result of transcallosal disinhibition (Andrews *et al.*, 1993; Rossini *et al.*, 2001; Jang, 2011). When the non- or less affected upper limb is also stimulated the relative difference in SEP response between the healthy and affected hemisphere could be examined, in addition to the absolute SEP response. Stimulation of the non- or less affected upper limb is therefore also included in the longitudinal study of the 4D-EEG project.

6 Conclusions

To conclude, the present study was able to reveal two subject-specific dipolar sources for the P50 and P100 SEP-components. No differences were found when the difference in location and orientation between the P50 and P100 source was compared between healthy subjects and chronic stroke patients. In contrast to the expectation, the sources for P50 and P100 were not consistently located in SI and SII, respectively. The predictive value of P50 and P100 for upper limb recovery post stroke remains therefore unclear and will be further evaluated in the longitudinal study of the 4D-EEG project. In this study it can be examined how the location, orientation and strength of the subject-specific P50 and P100 sources change over time in the early period post stroke and it can be examined how these changes are related to upper limb function. Moreover, when the required adjustments are made this study may be able to localize the P50 and P100 sources in, respectively, SI and SII.

7 Acknowledgements

I would like to thank my supervisors Caroline Winters, Erwin van Wegen and Andreas Daffertshofer for their time and feedback during my analysis and for the helpful comments on my final report. I would also like to thank Gert Kwakkel for the opportunity to perform my Research Internship in the 4D-EEG project. It was a pleasure to work in this project and I learned a lot from the EEG measurements in the survey van. In addition, thanks to Konstantina Kalogianni and Jan de Munck for their time to help me with the SEP analysis and to Mique Saes for the good cooperation during the past year.

8 References

- Allison, T., McCarthy, G., Wood, C.C., Darcey, T.M., Spencer, D.D., & Williamson, P.D. (1989a). Human cortical potentials evoked by stimulation of the median nerve. I. Cytoarchitectonic areas generating short-latency activity. *Journal of Neurophysiology*, 62, 694-710.
- Allison, T., McCarthy, G., Wood, C.C., Williamson, P.D., & Spencer, D.D. (1989b). Human cortical potentials evoked by stimulation of the median nerve. II. Cytoarchitectonic areas generating long-latency activity. *Journal of Neurophysiology*, 62, 711-722.
- Al-Rawi, M.A., Hamdan, F.B., & Abdul-Muttalib A.K. (2009). Somatosensory Evoked Potentials as a Predictor for Functional Recovery of the Upper Limb in Patients with Stroke. *Journal of Stroke Cerebrovascular Diseases*, 18, 262-268.
- Andrews, R.J., Bringas, J.R., Alonzo, G., Salamat, M.S., Khoshyomn, S., & Gluck, D.S. (1993). Corpus collosotomy effects on cerebral blood flow and evoked potentials (transcallosal dischisis). *Neuroscience Letters*, 154, 9-12.
- Babiloni, C., Pizzella, V., Del Gratta, C., Ferretti, A., & Romani, G.L. (2009). FUNDAMENTALS OF ELECTROENCEPHALOGRAPHY, MAGNETOENCEPHALOGRAPHY, AND FUNCTIONAL MAGNETIC RESONANCE IMAGING. *International Review of Neurobiology*, 86, 67-80.
- Benarroch, E.E. (2006). Basic neurosciences with clinical applications. Edinburgh: Butterworth Heinemann/Elsevier.
- Buchner, H., Fuchs, M., Wischmann, H., Dössel, Ludwig, I., Knepper, A., & Berg, P. (1994). Source Analysis of Median Nerve and Finger Stimulated Somatosensory Evoked Potentials: Multichannel Simultaneous Recording of Electric and Magnetic Fields Combined with 3D-MR Tomography. *Brain Topography*, 6, 299-310.
- Buchner, H., Knoll, G., Fuchs, M., Rienaäcker, A., Beckmann, R., Wagner, M., Silny, J., Jörg, P. (1997). Inverse localization of electric dipole current sources in finite element models of the human head. *Electroencephalography and Clinical Neurophysiology*, 102, 267- 278.
- Buma, F., Kwakkel, G., & Ramsey, N. (2013). Understanding upper limb recovery after stroke. *Restorative Neurology and Neurosciences*, 31, 707-722.
- Burton, H., Abend, N.S., MacLeod, A.M., Sinclair, R.J., Snyder, A.Z., & Raichle, M.E. (1999). Tactile attention tasks enhance activation in somatosensory regions of parietal cortex: a positron emission tomography study. *Cerebral Cortex*, 9, 662-674.
- Cruccu, G., Aminoff, M.F., Curio, G., Guerit, J.M., Kakigi, R., Mauguiere, F., Rossini, P.M., Treede, R.D., & Garcia-Larrea, L. (2008). Recommendations for the clinical use of somatosensory-evoked potentials. *Clinical Neurophysiology*, 119, 1705-1719.
- Desmedt, J.E., & Robertson D. (1977). Differential enhancement of early and late components of the cerebral somatosensory evoked potentials during forced-paced cognitive tasks in man. *The Journal of Physiology*, 271, 761-782.
- Disbrow, E., Roberts, T., & Krubitzer, L. (2000). Somatotopic organization of cortical fields in the lateral sulcus of Homo sapiens: Evidence for SII and PV. *Journal of Comparative Neurology*, 418, 1-21.
- Duncan, P.W., Propst, M., & Nelson, S.G. (1983). Reliability of the Fugl-Meyer assessment of sensorimotor recovery following cerebrovascular accident. *Physical Therapy*, 63, 1607-1610.
- Elbert, T., Junghöfer, M., Scholz, B., & Schneider, S. (1995). The Separation of Overlapping Neuromagnetic Sources in First and Second Somatosensory Cortices. *Brain Topography*, 7, 275-282
- Feijs, H., Van Hees, J., Bruyninckx, F., Mercelis, R., & De Weerd, W. (2000). Value of somatosensory and motor evoked potentials in predicting arm recovery after stroke. *Journal of Neurology, Neurosurgery and Psychiatry*, 68, 323-331.
- Fender, O.H. (1987). Source localization of brain electrical activity. In A.S. Gevins & A. Remond (Eds.), *Handbook of Electroencephalography and Clinical Neurophysiology*, Rev. Ser., Vol. 1: Methods of Analysis of Brain Electrical and Magnetic Signals (pp. 355-399). Elsevier.
- Forss, N., Hari, R., Salmelin, R., Ahonen, A., Hämäläinen, M., Kajola, M., Knuutila, J., & Simola, J. (1994). Activation of the human posterior parietal cortex by median nerve stimulation. *Experimental Brain Research*, 99, 309-315.
- Forss, N., & Jousmäki, V. (1998). Sensorimotor integration in human primary and secondary somatosensory cortices. *Brain Research*, 781, 259-267.
- Forss, N., Mustanoja, S., Roiha, K., Kirveskari, E., Mäkelä, J.P., Salonen, O., Tatlisumak, T., & Kaste, M. (2012). Activation in Parietal Operculum Parallels Motor Recovery in Stroke. *Human Brain Mapping*, 33, 534-541.
- Fuchs, M., Kastner, J., Wagner, M., Hawes, S., & Ebersole, J.S. (2002). A standardized boundary element method volume conductor model. *Clinical Neurophysiology*, 113, 702-712.
- Fugl-Meyer, A., Jääskö, L., Leyman, I., Olsson, S., & Stegling, S. (1975). The poststroke hemiplegic patient. Part I. A method for evaluation of physical performance. *Scandinavian Journal of Rehabilitation Medicine*, 7, 13-31.
- Hämäläinen, H., Kekoni, J., Sams, M., Reinikainen, K., & Näätänen, R. (1990). Human somatosensory evoked potentials to mechanical pulses and vibration: contributions of SI and SII somatosensory cortices to P50 and P100 components. *Electroencephalography and Clinical Neurophysiology*, 75, 13-21.
- Helmholtz, H. (1853). Über einige Gesetze der Vertheilung elektrischer Ströme in körperlichen Leitern, mit Anwendung auf die thierisch-elektrischen Versuche. *Annalen der Physik und Chemie*, 29, 222-227.
- Hendricks, H.T., Pasma, J.W., Mulder, T., Notermans, S.L., & Schoonderwaldt, H.C. (1994). The value of somatosensory evoked potentials for the prediction of motor recovery of the upper extremity after cerebral infarction. *Journal of Rehabilitation Sciences*, 7, 3-8.

- Hendricks, H.T., Hageman, G.T.P., & van Limbeek, J. (1997). Prediction of recovery from upper extremity paralysis after stroke by measuring evoked potentials. *Scandinavian Journal of Rehabilitation Medicine*, 29, 155-159.
- Hendricks, H.T., van Limbeek, J., Geurts, A.C., & Zwartz, M.J. (2002). Motor Recovery After Stroke: A Systematic Review of the Literature. *Archives of Physical Medicine and Rehabilitation*, 83, 1629-1637.
- Hollander, M., Koudstraal, P.J., Bots, M.L., Grobbee, D.E., Hofman, A., & Breteler, M.M.B. (2003). Incidence, risk, and case of fatality of first ever stroke in the elderly population. The Rotterdam Study. *Journal of Neurology, Neurosurgery and Psychiatry*, 74, 317-321.
- Hossmann, K.A. (2006). Pathophysiology and therapy of experimental stroke. *Cellular and Molecular Neurobiology*, 26, 1057-1083.
- Hu, L., Zhang, Z.G., & Hu, Y. (2012). A time-varying source connectivity approach to reveal human somatosensory information processing. *NeuroImage*, 62, 217-228.
- Jang, S.H. (2011). Contra-lesional somatosensory cortex activity and somatosensory recovery in two stroke patients. *Journal of Rehabilitation Medicine*, 43, 268-270.
- Jones, E.G., Coulter, J.D., & Hendry, S.H.C. (1978). Intracortical connectivity of architectonic fields in the somatic sensory motor and parietal cortex of monkeys. *Journal of Comparative Neurology*, 181, 291-348.
- Inui, K., Wang, X., Tamura, Y., Kaneoke, Y., & Kakigi, R. (2004). Serial Processing in the Human Somatosensory System. *Cerebral Cortex*, 14, 851-857
- Karhu, J., & Tesche, C.D. (1999). Simultaneous Early Processing of Sensory Input in Human Primary (SI) and Secondary (SII) Somatosensory Cortices. *Journal of Neurophysiology*, 81, 2017-2015.
- Keren, O., Ring, H., Solzi, P., Pratt, H., & Groswasser, Z. (1993). Upper Limb Somatosensory Evoked Potentials as a Predictor of Rehabilitation Progress in Dominant Hemisphere Stroke Patients. *Stroke*, 24, 1789-1793.
- van Kordelaar, J., van Wegen, E.E.H., Nijland, R.H.M., de Groot, J.H., Daffertshofer, A., & Kwakkel, G. (2013). Understanding Adaptive Motor Control of the Paretic Upper Limb Early Poststroke: The EXPLICIT-stroke Program. *Neurorehabilitation and Neural Repair*, 27, 854-863.
- Kwakkel, G., Kollen, B., & Twisk, J. (2006). Impact of time on improvement of outcome after stroke. *Stroke*, 37, 2348-2353.
- van der Lee, J.H., Roorda, L.D., Beckerman, H., Lankhorst, G.J., & Bouter, L.M. (2002). Improving the Action Research Arm test: a unidimensional hierarchical scale. *Clinical Rehabilitation*, 16, 646-653.
- Lyle, R.C. (1981). A performance test for assessment of upper limb function in physical rehabilitation treatment and research. *International Journal of Rehabilitation Research*, 4, 483-92.
- Nijland, R.H.M., van Wegen, E.E.H., Harmeling-van der Wel, B.C., Kwakkel, G. (2010). Presence of Finger Extension and Shoulder Abduction Within 72 hours After Stroke Predicts Functional Recovery. Early Prediction of Functional Outcome After Stroke: The EPOS Cohort Study. *Stroke*, 41, 745-750.
- Mauguière, F., Allison, T., Babiloni, C., Buchner, H., Eisen, A.A., Goodin, D.S., Jones, S.J., Kakigi, R., Matsuoka, S., Nuwer, M., Rossini, P.M., & Shibasaki, H. (1999). Recommendations for the Practice of Clinical Neurophysiology: Guidelines of the International Federation of Clinical Physiology. *Electroencephalography and Clinical Neurophysiology*, 52, 3-304.
- Mima, T., Nagamine, T., Nakamura, K., & Shibasaki, H. (1998). Attention Modulates Both Primary and Secondary Somatosensory Cortical Activities in Humans: A Magnetoencephalographic Study. *Journal of Neurophysiology*, 80, 2215-2221
- Mosher, J.C., Lewis, P.S., & Leahy, R.M. (1992). Multiple dipole modeling and localization from spatio-temporal MEG data. *IEEE Transactions on Biomedical Engineering*, 39, 541-557.
- Murphy, T.H., & Corbett, D. (2009). Plasticity during stroke recovery: from synapse to behaviour. *Nature Reviews Neuroscience*, 10, 861-872.
- Nunez, P. (1981). Quantitative states of neocortex. In: Nunez, P. (Ed.), *Neocortical Dynamics and Human EEG Rhythms*. Oxford University Press, Inc., New York, pp. 3 - 67.
- Nuwer, M.R. (1998). Fundamentals of evoked potentials and common clinical applications today. *Electroencephalography and clinical Neurophysiology*, 106, 142-148.
- O'Donnell, R. D., Berkhout, J., & Adey, W. R. (1974). Contamination of scalp EEG spectrum during contraction of craniofacial muscles. *Electroencephalography and Clinical Neurophysiology*, 37, 145-151.
- Oostenveld, R., Fries, P., Maris, E., & Schoffelen, J. (2011). Fieldtrip: Open Source Software for Advanced Analysis of MEG, EEG, and Invasive Electrophysiological Data. *Computational Intelligence and Neuroscience*, Volume 2011, Article ID 156869, 9 pages doi:10.1155/2011/156869.
- Péron, Y., Aubertin, P., & Guihéneuc, P. (1995). Prognostic significance of electrophysiological investigations in stroke patients: somatosensory and motor evoked potentials and sympathetic skin response. *Clinical Neurophysiology*, 25, 146-157.
- Ploner, M., Schmitz, F., Freund, H., & Schnitzler, A. (2000). Differential Organization of Touch and Pain in Human Primary Somatosensory Cortex. *Journal of Neurophysiology*, 83, 1770-1776.
- Pons, T.P., Garraghty, P.E., & Mishkin, M. (1988). Lesion-induced plasticity in the second somatosensory cortex adult macaques. *PNAS*, 85, 5279-5281.
- Roosink, M., Buitenweg, J.R., Renzenbrink, G.J., Geurts, A.C.H., & IJzerman, M.J. (2011). Altered cortical somatosensory processing in chronic stroke: A relationship with post-stroke shoulder pain. *NeuroRehabilitation*, 28, 331-344.
- Rossini, P.M., Tecchio, F., Pizzella, V., Lupoi, D., Cassetta, E., & Paqualetti, P. (2001). Interhemispheric Differences in Sensory Hand Areas after Monohemispheric Stroke: MEG/MRI Integrative Study. *NeuroImage*, 14, 474 - 485.
- Rothwell, J.C., Traub, M.M., Day, B.L., Obeso, J.A., Thomas, P.K., & Marsden, C.D. (1982). Manual motor performance in a

- deafferented man. *Brain*, 105, 515-442.
- Rothi, L.J., & Horner, J. (1982). Restitution and substitution: Two theories of recovery with application to neurobehavioral treatment. *Journal of Clinical Neurophysiology*, 51, 73- 81.
- Savitzky, A., & Golay, M.J.E. (1964). Smoothing and differentiation of data by simplified least-squares procedures, *Analytical Chemistry*, 36, 1627-1639.
- Scherg, M. (1990). Fundamentals of Dipole Source Potential Analysis. In F. Grandori, M. Hoke and G.L. Romani (Eds.), *Auditory Evoked Magnetic Fields and Electric Potentials. Advances in Audiology* (vol 6, pp: 40-69). Basel: Karger.
- Schnitzler, A., & Ploner, M. (2000). Neurophysiology and neuroanatomy of pain perception. *Journal of Clinical Neurophysiology*, 17, 592-603.
- Simoes, C., Mertens, M., Forss, N., Jousmaki, V., Lutkenhoner, B., & Hari, R. (2001). Functional overlap of finger representations in human SI and SII cortices. *Journal of Neurophysiology*, 86, 1661-1665.
- Timmerhuis, T.P.J., Hageman, G., Oosterloo, S.J., & Rozeboom, A.R. (1996). The prognostic value of cortical magnetic stimulation in acute middle cerebral artery infarction compared to other parameters. *Clinical Neurology and Neurosurgery*, 98, 231-236.
- Tzvetanov, P., & Rousseff, R.T. (2003). Median SSEP changes in hemiplegic stroke: Long-term predictive values regarding ADL recovery. *NeuroRehabilitation*, 18, 317-324.
- Ward, J.H., Jr. (1963). Hierarchical Grouping to Optimize an Objective Function. *Journal of the American Statistical Association*, 58, 236-244.
- Woolsey, C.N., Erikson, T.C., & Gilson, W.E. (1979). Localization in somatic and motor areas of human cerebral cortex as determined by direct recording of evoked potentials and electrical stimulation. *Journal of Neurosurgery*, 51, 476-506.
- Yuya, H., Nagata, K., Takanashi, Y., Satoh, Y., Watahiki, Y., Hirata, Y., Yokoyama, E., & Buchan, R.J. (1996). Scalp topography of SEP late components in patients with supra-tentorial lesions. *Brain Topography*, 8, 333-336.